On the Delicate State of Instability of a Vertical Riser Transporting Fluid

Hyung-Taek Kim[a], Oliver M. O'Reilly[a,*]

[a]*Department of Mechanical Engineering, University of California at Berkeley, Berkeley CA 94720, USA*

Abstract

The variation in the dynamic characteristics of a flexible riser as the riser transitions from a vertical riser to a catenary-type riser is investigated. It is well known that the straight configuration of a flexible vertical riser conveying fluid destablizes in a divergence-type instability once the velocity of the transporting fluid exceeds a critical speed. As expected, the instability persists if a slight horizontal offset is introduced at the hang-off point. However, as demonstrated in this paper, if a finite horizontal offset is introduced then the instability vanishes and the resulting static configuration of the catenary-type riser is stable regardless of the transport speed of the fluid.

Keywords: flexible riser, top end horizontal offset, Kirchhoff's rod theory, stability, top tension, internal fluid transport,

1. Introduction

The subject of this paper is the dynamics of a riser that transports fluid from the seabed to and from a moored vessel. Referring to Figure 1(a), if the hang-off point $\mathcal{H}$ is directly above the mooring point (or well head) $\mathcal{O}$ and the riser is vertical, then it is well known that the straight equilibrium configuration of the riser will become unstable if the speed of the fluid being transported by the riser is sufficiently large. If the hang-off point $\mathcal{H}$ is displaced so as to produce a so-called top end offset, then it is easy to deduce that the equilibrium configuration of the riser assumes the shape of a catenary. Indeed for a given value of the so-called top tension at the hang-off point, it is possible to have two configurations of the catenary-type riser (cf. Figure 1(b)).[1] The configuration with the shorter length is stable while the configuration with the longer length is unstable when fluid transport is considered. What is not understood is how an unstable vertical riser (labelled v in Figure 1(b)) can be stabilized as a catenary-type riser (labelled i in Figure 1(b)) for all fluid transport speeds when a horizontal offset is introduced. The purpose of the present paper is to resolve this issue and to explain the remarkable transition to stability that occurs when the horizontal offset is increased from zero. Our analysis

*Corresponding author, Tel.: +1 510 642 0877, oreilly@berkeley.edu

[1]The use of top tension to help classify the configurations of the riser is due to Chucheepsakul and his coworkers (see, e.g., Chucheepsakul and Monprapussorn (2001)).

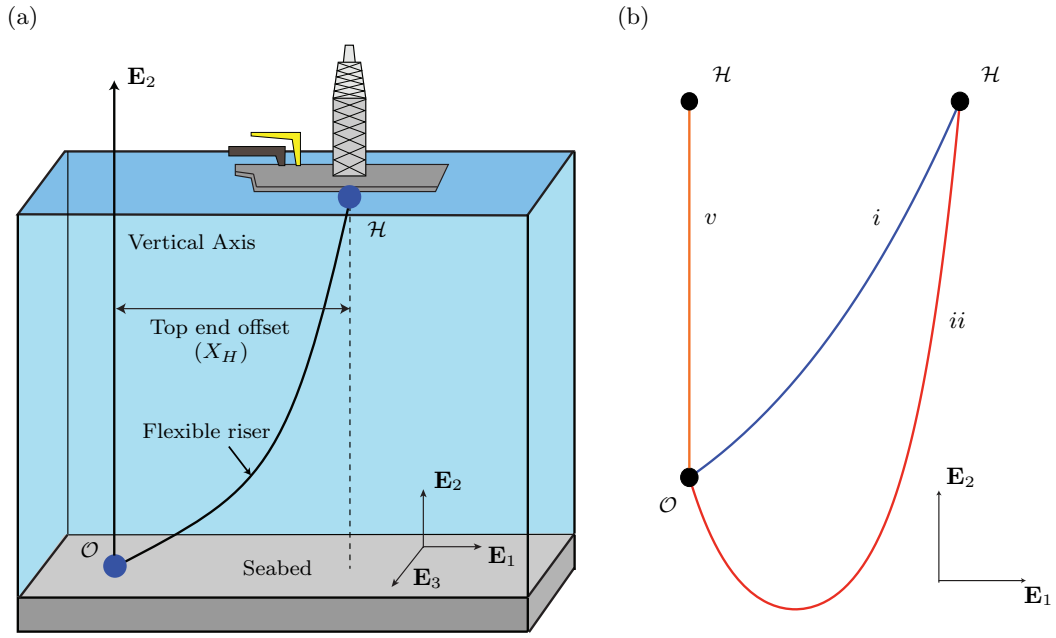

Fig. 1. (a) Flexible riser used in marine environments for oil and gas development process, which has a non-zero top end horizontal offset (X_H) from the vertical axis; and (b) three static riser configurations that have the identical magnitude of tension at the hang-off point $\mathcal{H}$. Previous work by Monprapussorn et al. (2007) showed that the vertical riser labeled v can experience a divergence-type instability. Our earlier work (Kim and O'Reilly (2019a)) established that the shorter riser, which is labeled i, is stable while the longer riser, which is labeled ii, can only become unstable in a flutter-type instability provided the effects of fluid transport in the riser are included in the model.

assumes that the top tension remains constant and the length of the undeformed riser changes accordingly.

An outline of this paper is as follows. In the next section, a brief review of the literature on divergence-type instability of vertical risers is presented. This review is complemented by a related discussion on catenary-type risers. The model for the riser and the numerical schemes used to solve the boundary-value problem for the static configuration and the linear vibration analysis are summarized in Section 3. A summary of the dynamics of the riser when a horizontal offset is introduced is presented in Section 4 and the main results of the paper are summarized in Section 5.

2. Background on Stability of Risers

By way of background, research on the destabilizing effects of internal flow on the dynamics of pipeline dates to the pioneering work by Païdoussis (1966). Surveys of this field, including discussion of the wide range of applications, can be found in Ibrahim (2010), Ibrahim (2011), Païdoussis (2014), and Païdoussis (2016). The vast majority of works in this area consider a straight pipe. For example, Ni et al. (2011) investigated the effects of the boundary conditions on the instabilities in a straight riser that are

present as the internal fluid speed is increased (quasistatically). They demonstrated that the instability was either a divergence type or flutter type depending on the boundary conditions. Their work also inspired the related investigations by Chang and Modarres-Sadeghi (2014), Ritto et al. (2014), and Sazesh and Shams (2019).

Extending the aforementioned works to catenary-type risers is challenging because the equilibrium configuration is not trivial. As a result, recourse to numerical methods must be made. However, considerable progress has been made in understanding the dynamics of catenary-type risers (cf. Chucheepsakul et al. (2003), Santillan et al. (2010), and Chatjigeorgiou (2010)). In particular, stability criteria for the catenary-type riser and the destabilizing effects of fluid flow are now more fully understood (cf. Kim and O'Reilly (2019a)). One aspect that has not been reported previously is the stabilization of a vertical riser, such as the configuration labelled v shown in Figure 1(b), when a sufficient large horizontal offset is introduced. The analysis in the present paper demonstrates how stabilization occurs. We show that the stability characteristics of a catenary-type riser whose horizontal offset is non-zero, such as the configuration labelled i in Figure 1(b), are noticeably different from the phenomenon observed for a vertical riser. For example, the vertical riser has a critical speed of internal flow at which the lowest natural frequency of the riser drops down to zero and a divergence-type instability occurs, while the catenary-type riser can remain stable regardless of the fluid transport speed. Additionally, we will show how the modal analysis for the vertical riser and the catenary-type riser can also be dramatically different. To provide this explanation, we found that we needed to extend and complement earlier works such as Klaycham et al. (2017) and Alfosail et al. (2017) by considering both in-plane and out-of-plane modes and fluid transport.

3. Modeling a Flexible Riser

As may be seen from the literature, flexible risers are modeled using a variety of string and rod theories and finite element methods. In the work presented here, we will use the rod-based model discussed in Kim and O'Reilly (2019a). The rod theory used for this model is known as Kirchhoff's rod theory. The theory accommodates non-planar motions of the rod and is able to model extension, bending, and torsion of the rod as is discussed in a number of books including Antman (2005), Love (1927), and O'Reilly (2017). Referring to Fig. 1(a), the rod is assumed to be submerged in a fluid. Thus, in addition to a gravitational force, a buoyancy force and the effects of an external current are modeled. The prescriptions for the drag and added mass forces are obtained from the generalized Morison equation (Morison et al. (1950)). Furthermore, the effects of transporting a fluid at a constant speed V_i inside the riser is also included. The parameter values for the riser considered in the present paper are summarized in Table 1. In the interests of brevity, we do not repeat the lengthy formulation of the equations of motion and solution procedures and instead refer the interested reader to the paper Kim and O'Reilly (2019a).

After formulating the boundary-value problem, the static configuration of the rod is computed directly using the MATLAB built-in function 'bvp4c' which is a finite difference code that implements the 3-stage Lobatto IIIa formula (Shampine et al. (2003)). Among others, the static (equilibrium) configuration will depend on the fluid transport speed, the buoyancy force on the riser, and the horizontal offset. To examine the stability of a static configuration, we consider small amplitude perturbations to the static configuration

Table 1. The values of the parameters used for the riser model in our numerical analyses.

Parameter[a]	Symbol	Unit	Values
density of sea water	ρ_f	kg/m^3	1025
density of internal fluid	ρ_i	kg/m^3	998
density of riser	ρ_o	kg/m^3	7850
outer diameter	D_o	m	0.26
inner diameter	D_i	m	0.20
cross-sectional area of outer pipe $A_o = \pi\left(D_o^2 - D_i^2\right)/4$	A_o	m^2	2.17×10^{-2}
cross-sectional area of inner pipe[b] $A_i = \pi D_i^2/4$	A_i	m^2	3.14×10^{-2}
horizontal offset	X_H	m	0
vertical offset	H	m	300
bending stiffness[c]	EI	Nm^2	3.02×10^7
axial stiffness	EA	N	4.49×10^9
added mass coeff.	C_a	-	1.0
normal drag coeff.	C_n	-	0.7
tangential drag coeff.	C_t	-	0.03
prespecified top tension	T_H	kN	476.2
internal fluid speed	V_i	m/s	$0 - 100$
external current speed	V_F	m/s	0
gravitational constant	g	m/s^2	9.81

[a] Monprapussorn et al. (2007).
[b] This is the cross-sectional area of the riser through which the fluid is transported.
[c] The area moment of inertia $I = \pi/64\left(D_o^4 - D_i^4\right)$.

using a standard procedure (see, for example, Neukirch et al. (2012)). With the help of the boundary conditions, we compute eigenvalues and corresponding eigenmodes of the static configuration of the riser. The eigenvalues are expressed as follows:

$$\lambda_n = \mathrm{Re}\left(\lambda_n\right) + i\mathrm{Im}\left(\lambda_n\right) = \delta_n + i\omega_n. \tag{3.1}$$

Classic results (see, for example, Atanackovic (1997)) are then used to determine the linear stability of the static configuration of the riser. In particular, if the real part of a single λ_n is positive, then the static configuration is said to be (linearly) unstable. Otherwise, when $\delta_n \leq 0$ for all n, then the static configuration is said to be linearly stable. That is, small perturbations to the static configuration do not lead to unbounded motions of the riser.

4. Numerical results and parametric studies

4.1. Validations of Model and Solution Procedures

Prior to examining the effects of the horizontal offset on the dynamic characteristics and the stability of the riser, we validated our method to compute the static configurations and variation of natural frequencies with changes to the internal fluid speed. To this end, we compared our predicted results with those from Païdoussis (1975) for

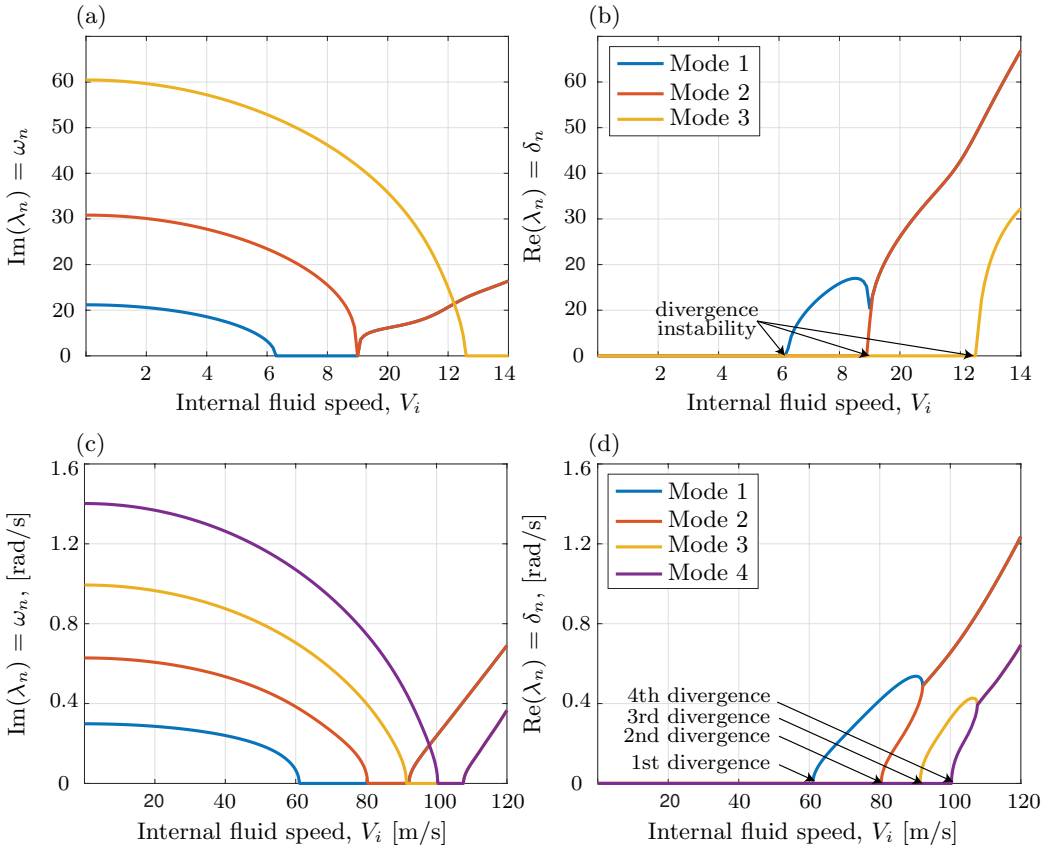

Fig. 2. The variation of the lowest modes for two types of riser: (a) and (b), a clamped-clamped horizontal pipe; and (c) and (d), a vertical riser. (a) and (c) show the natural frequencies of the lowest modes, i.e., imaginary part of eigenvalues (ω_n), while (b) and (d) show the real part of the first three (four) eigenvalues (δ_n) and can be used to deduce information concerning stability of the static configuration. The parameter values for the pipe are taken from Païdoussis (1975) and Païdoussis (2014)[Section 3.4.1], The parameter values for the vertical riser are presented in Table 1 and are adapted from Monprapussorn et al. (2007).

a clamped-clamped horizontal pipe[2] and Monprapussorn et al. (2007) who considered a pinned-pinned vertical riser. As can be seen from Fig. 2, our results are in good agreement for both types of model. In addition, we see that there exists a critical velocity where a divergence-type instability occurs. As the speed of internal fluid transport V_i keeps increasing, the first and second modes merge, and the third and fourth modes also merge.

4.2. The effects of the horizontal offset X_H when the effects of the internal fluid are omitted

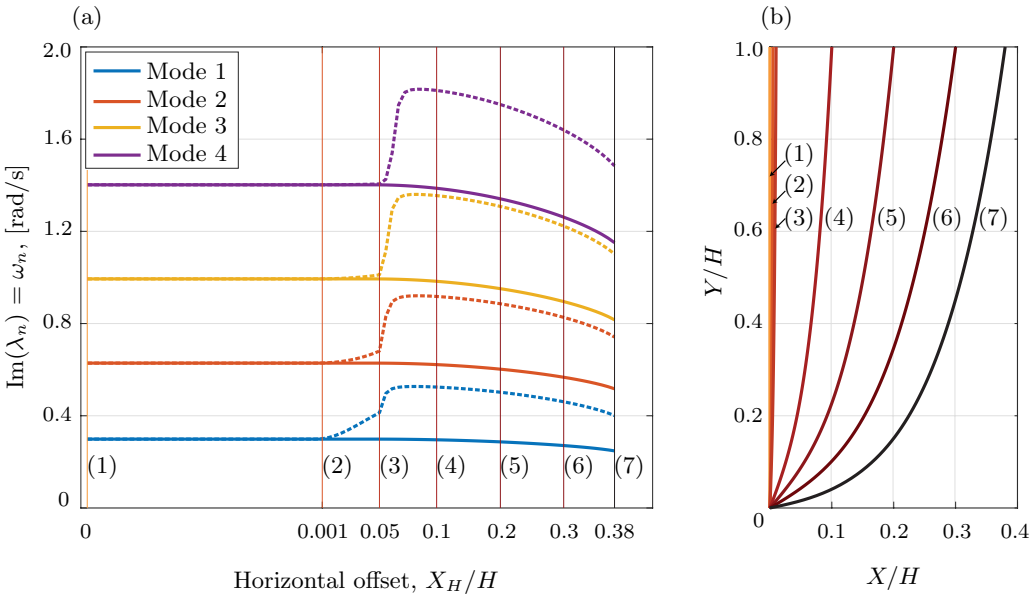

Fig. 3. (a) Variation of ω_n for the lowest four out-of-plane modes (solid lines), and in-plane modes (dashed lines) with increasing dimensionless horizontal offset X_H/H; and (b) static equilibrium configurations corresponding to distinct values of X_H/H: (1) 0; (2) 0.001; (3) 0.05; (4) 0.1; (5) 0.2; (6) 0.3; and (7) 0.38.

After validating our results with previous works, we performed a series of numerical analyses to determine the quantitative effects of the horizontal offset on the dynamic response of the riser. For our model, we used the same parameter values as those in Monprapussorn et al. (2007) that are listed in Table 1. Of particular interest to us in this paper are solutions with pinned boundary conditions in dimensionless form applied at the ends $\mathcal{O}$ and $\mathcal{H}$ of the riser as follows:

$$\begin{aligned} &\text{At } \mathcal{O}: x = 0, \quad y = 0, \quad z = 0, \quad \bar{\nu}_1 = 0, \quad \bar{\nu}_2 = 0, \quad \bar{\nu}_3 = 0, \\ &\text{At } \mathcal{H}: x = x_H, \quad y = y_H, \quad z = z_H, \quad \bar{\nu}_1 = 0, \quad \bar{\nu}_2 = 0, \quad \bar{\nu}_3 = 0. \end{aligned} \tag{4.1}$$

[2]This work is also summarized in Païdoussis (2014) along with many other applications.

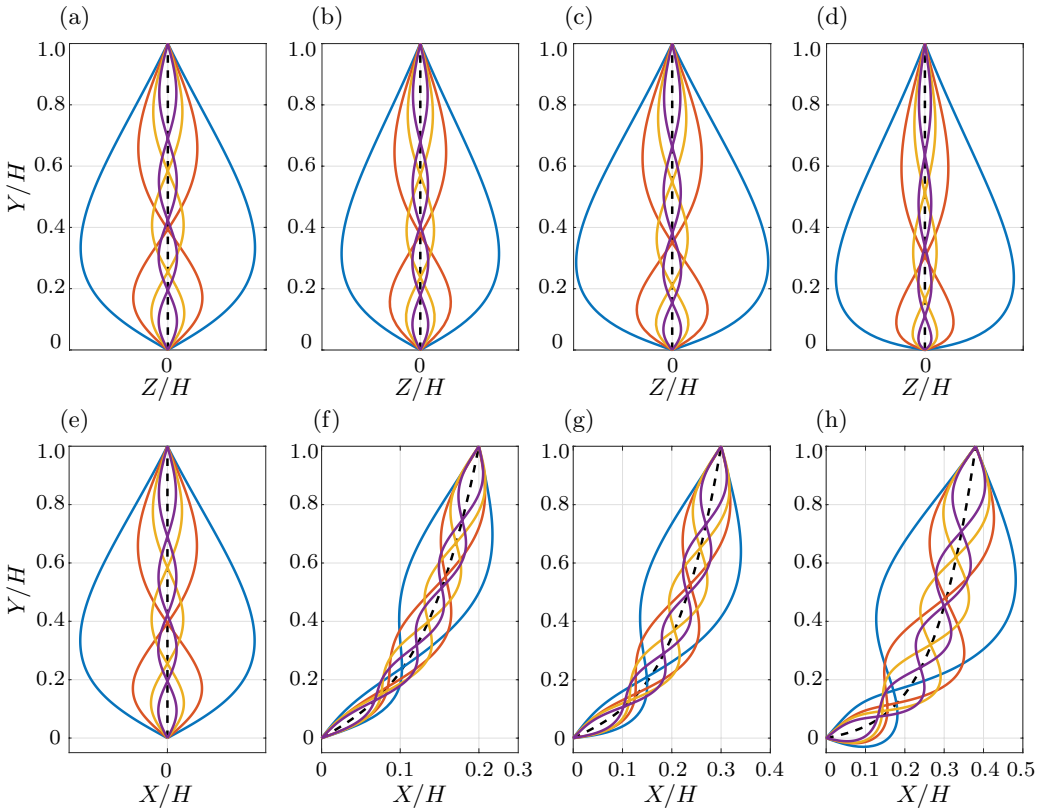

Fig. 4. The mode shapes of the lowest four out-of-plane bending modes in the YZ plane for various values of X_H/H: ((a) 0; (b) 0.2; (c) 0.3; and (d) 0.38), and in-plane bending modes in the XY plane for various values of X_H/H: ((e) 0; (f) 0.2; (g) 0.3; and (h) 0.38).

Here, $\bar{\nu}_{1,2}$ are bending strains and $\bar{\nu}_3$ is the torsional strain in the rod, which correspond to the bending and torsional moment, respectively.

After solving the static equations, the modal characteristics of the riser are investigated. Our first set of analyses ignored the effects of the transported fluid. That is, the transport speed is set to zero ($V_i = 0$). We then extended the work of Monprapussorn et al. (2007) by considering both out-of-plane and in-plane vibrations of the riser simultaneously. The variation of the lowest four out-of-plane modes and in-plane modes are shown in Fig. 3(a). The companion Fig. 3(b) shows static equilibrium configurations for several values of the horizontal offset. It should be noted that as the horizontal offset is increased, the magnitude of top tension is kept constant ($T_{Top} = 476.2$ kN) and the length of the undeformed riser is increased accordingly. Referring to Fig. 3(b), when the offset (X_H/H) is less than 10^{-3}, the out-of-plane and in-plane modes are practically identical. Because the rod modeling the riser is assumed to be isotropic ($EI_1 = EI_2$), these results are anticipated. As the horizontal offset is increased, however, it is interesting to note that the eigenvalues associated with out-of-plane modes on the YZ plane and the in-plane modes on the XY plane begin to separate. That is, as X_H increases

and the curvature on the XY plane ν_1 becomes increasingly non-uniform, the isotropy of the rod is insufficient for the two sets of modes to remain similar. For the riser with a sufficiently large horizontal offset, for example $X_H/H > 0.01$, the natural frequencies of the out-of-plane modes and in-plane modes are remarkably different, as we can see from the considerable difference between the solid and dashed lines for each mode in Fig. 3(a) for large values of X_H/H.

The mode shapes of the lowest four out-of-plane modes on the YZ plane are shown in Fig. 4(a)-(d), and the corresponding in-plane modes are shown in Fig. 4(e)-(h) for several distinct values of the horizontal offset X_H/H. As can be deduced from those figures, the out-of-plane mode shapes are invariant under changes in X_H, while in-plane mode shapes show noticeable changes as X_H/H is increased from 0. As the curvature ν_1, which is initially zero for the vertical riser, becomes increasingly nonuniform, the static configuration looses symmetry and the riser becomes stiffer in-plane compared to out-of-plane. Accordingly, the two types of modes become increasingly distinct. Further, the natural frequencies of in-plane modes increase while those of out-of-plane modes do not change significantly.

Referring to the in-plane modes (i.e., the modes on the XY plane) for the riser that has non-zero horizontal offset shown in Fig. 4(f)-(h), we observed that the fundamental mode appears at first glance to be akin to a second mode that has a nodal point along the static configuration. Additionally, the second mode appears to be a third mode with a pair of nodal points, and so on. However, this illusion can be attributed to the fact that the mode shapes are superposed on static configurations that have significant curvatures. We take this opportunity to note that similar results for the deformed mode shape have been reported by Bylsma et al. (1988) for a simple suspended chain and Eroglu and Tufekci (2018) for a highly deformed beam.

As discussed in our earlier works (Kim and O'Reilly (2019a,b)), the modes for the static configurations are always stable so long as the internal fluid speed V_i is set to zero. Thus, all the static solutions shown in Fig. 1(b) and those shown in Fig. 3(b) are linearly stable regardless of the values of horizontal offset (X_H/H).

4.3. The effects of a horizontal offset when an internal fluid is being transported

In this section, the effects of the horizontal offset X_H on the dynamic characteristics and stability of the riser as the speed of transport V_i of the internal fluid is varied are discussed. Fig. 5 shows the variation of the natural frequencies of the lowest four out-of-plane and in-plane bending modes at several distinct values of the horizontal offset. As mentioned previously, as the hang-off point moves further away from the zero offset position, the out-of-plane and in-plane bending modes become distinct when the riser has a horizontal offset of 3×10^{-6} (cf. Fig. 5(c)) or higher (cf. Fig. 5(d)-(i)). [3] As can be inferred from Fig. 5(c)-(d), for equilibrium configurations with the horizontal offset ranging from 3×10^{-6} to 3×10^{-5}, the separation of the out-of-plane and in-plane modes takes place at 61.1 m/s, i.e., the critical velocity at which the first mode of the vertical riser (Fig. 5(a)) or near vertical riser (Fig. 5(b)) destabilizes. As the offset keeps increasing, the velocity at which the separation of the two types of modes is triggered continues to decrease (cf. Fig. 5(e)-(f)). Thus, the configurations with significant values

[3] It is noted that the precision of bvp4c solver is 16 digits, as a default value provided by Matlab.

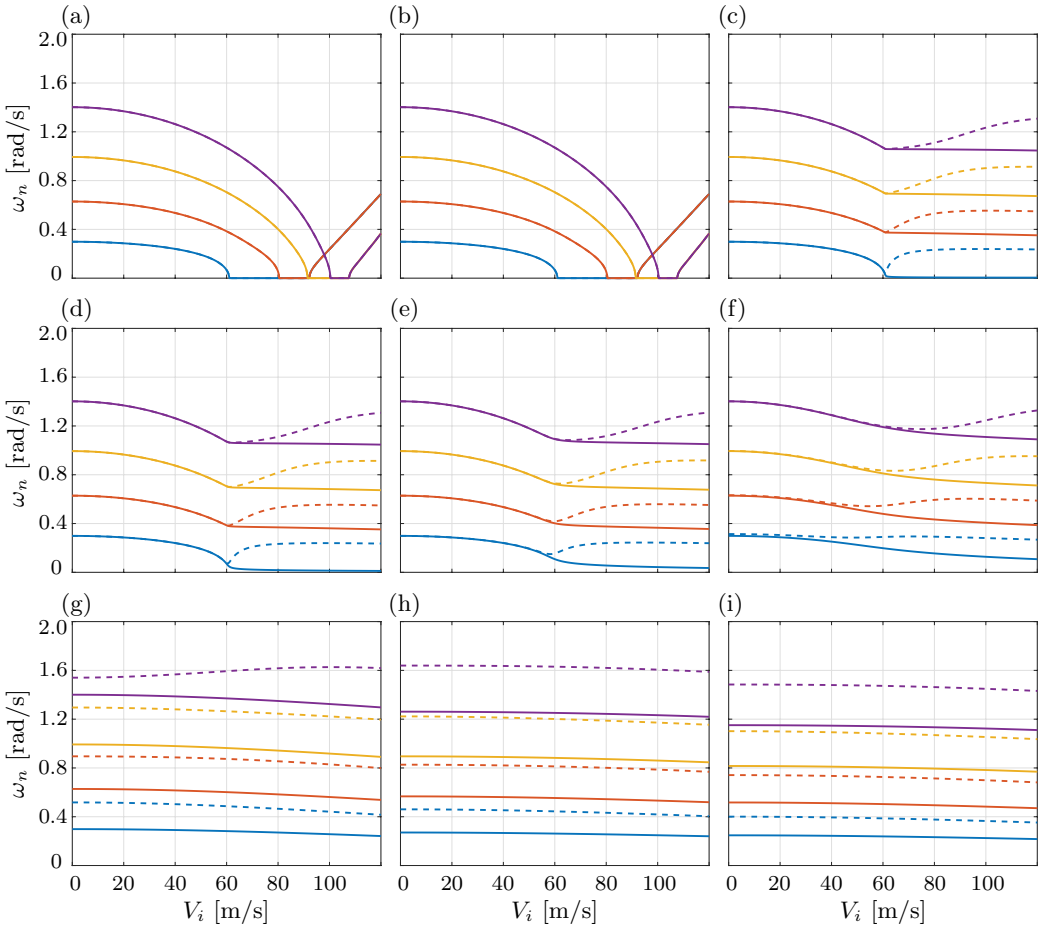

Fig. 5. The variations in the natural frequencies (ω_n) of the lowest four bending modes as a function of the transport speed V_i of the internal fluid for various values of the dimensionless horizontal offset (X_H/H): (a) 0 (Vertical riser); (b) 3×10^{-7}; (c) 3×10^{-6}; (d) 3×10^{-5}; (e) 3×10^{-4}; (f) 3×10^{-3}; (g) 0.03; (h) 0.3; and (i) 0.38. For the results shown in (a), the critical speed of internal fluid transport for the onset of instabilities are listed in Table 2. The solid lines show the out-of-plane bending modes while the dashed lines show the in-plane bending modes.

of horizontal offset such as Fig. 5(g)-(i) have distinct modal characteristics for the out-of-plane and in-plane modes as soon as the fluid is being internally transported. This observation is consistent with the findings discussed in the previous section.

As regards the stability of the static configurations when the transport of the internal fluid with non-zero speed is taken into account, it should be noted that all of the out-of-plane and in-plane modes shown in Fig. 5 are stable except for two cases ((a) and (b)). That is, the real part of the eigenvalues are nearly zero and negative as shown in Fig. 6. For the results shown for the vertical riser and nearly vertical riser ($X_H/H < 6 \times 10^{-7}$) in Fig. 5(a)-(b), and Fig. 6(a)-(b), it is apparent that critical velocity values exist where the corresponding modes become unstable. It should be noted that the value

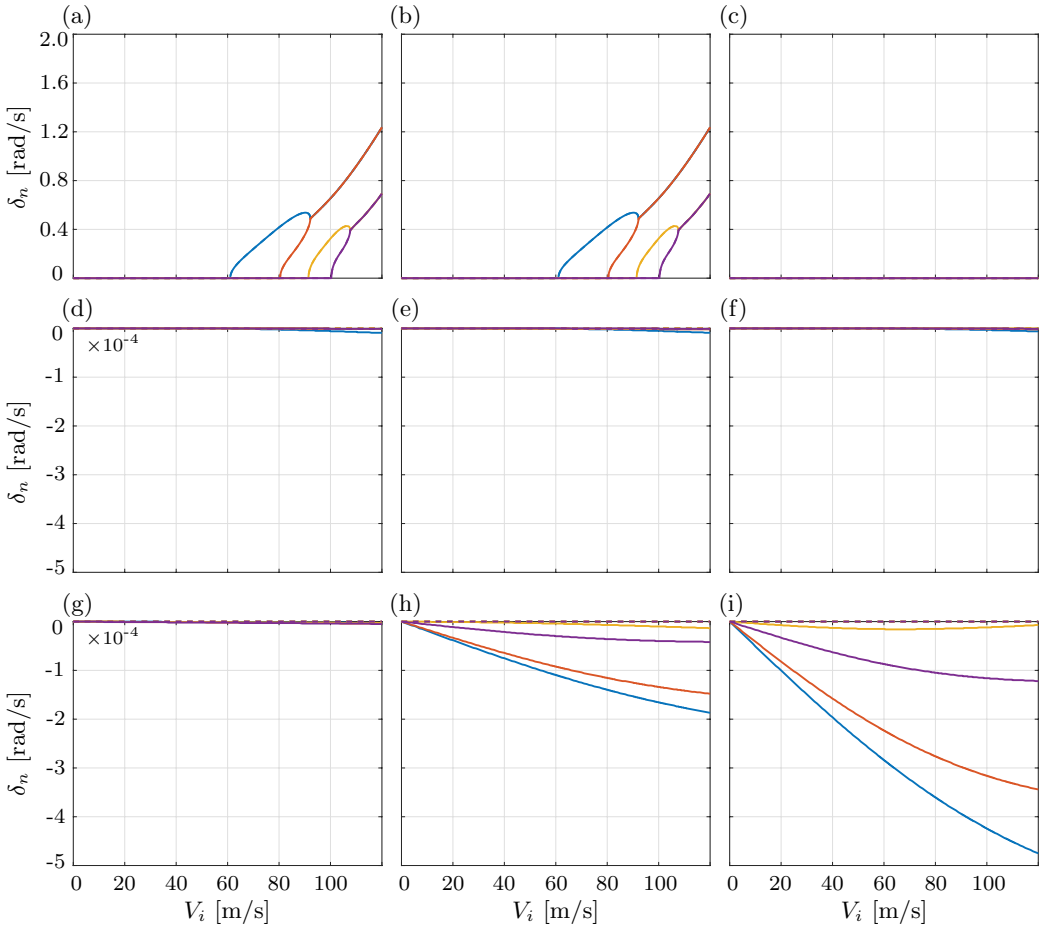

Fig. 6. The variations of the real part of the eigenvalues (δ_n) of the lowest four bending modes as a function of the transport speed V_i of the internal fluid for various values of the dimensionless horizontal offset (X_H/H): (a) 0 (Vertical riser); (b) 3×10^{-7}; (c) 3×10^{-6}; (d) 3×10^{-5}; (e) 3×10^{-4}; (f) 3×10^{-3}; (g) 0.03; (h) 0.3; and (i) 0.38. The solid lines show the out-of-plane bending modes while the dashed lines show the in-plane bending modes.

$X_H/H = 6 \times 10^{-7}$ is the exact point captured by our numerical methods where the separation of th out-of-plane modes and in-plane modes occurs. The results shown in Fig. 5(b), and Fig. 5(c), which correspond to the horizontal offsets $X_H/H = 3 \times 10^{-7}$, and $X_H/H = 3 \times 10^{-6}$, respectively, are displayed in order to highlight the separation that starts to occur when $X_H/H = 6 \times 10^{-7}$.

We interpret the case where the hang-off point is given a small ($X_H/H < 6 \times 10^{-7}$) displacement as a perturbation of the vertical riser. The results for this case show that when fluid is being transported at a speed beyond the critical speed, then the vertical riser is unstable both to perturbations that satisfy the boundary conditions and those that perturb the hang-off point.

We conclude that for risers that have vertical equilibrium configurations (i.e., vertical

risers), instability at a critical value of the fluid transport speed is inevitable. Right beyond this point, however, finite values of the horizontal offset produce stable static configurations that are almost vertical and thus similar in appearance to a vertical riser (cf. Fig. 3(b)). For instance, for the offset $X_H/H = 3 \times 10^{-6}$, instead of becoming unstable as the transport speed V_i of the internal fluid is increased, the out-of-plane and in-plane modes separate and remain stable (cf. Fig. 5(c)) as the dimensionless horizontal offset is increased to 0.38,[4] both the lowest four out-of plane and in-plane modes remain stable (cf. Fig. 6(d)-(f)).

Our results are in agreement with our earlier work (Kim and O'Reilly (2019a)). In that paper, we showed that a catenary-type flexible riser with a non-zero horizontal offset remains stable (even when the effects of fluid transport are considered) provided the static configuration is the shorter of the two configurations having the same value of top tension (T_{Top}) and the prescribed top tension is above the critical top tension.

Table 2. The speed of internal fluid at which instability occurs.

Type of instability	Divergence				Flutter[a]	
	1st	2nd	3rd	4th	1st	2nd
Critical internal fluid speed [V_i, m/s]	61.1	80.5	91.5	100.4	92.2	107.7

[a] Flutter-type instability is found with combinations of modes, i.e., the 1st flutter instability involves the 1st and 2nd bending modes, and the 2nd flutter instability features the 2nd and 3rd bending modes.

4.4. The effects of internal fluid speed

Since the effects of internal fluid on the stability of both vertical risers and catenary-type risers have now been described, we now focus attention on the sudden change in stability characteristics as X_H/H is varied. The results shown in Fig. 7, and Fig. 8 demonstrate, respectively, the variation of imaginary (ω_n) and real (δ_n) parts of the lowest four eigenvalues as X_H/H increases for distinct values of the internal fluid speed V_i.

As can be seen in Fig. 7(a)-(c) and Fig. 8(a)-(c), as long as V_i is below the critical speed 61.1m/s for a vertical riser, the riser remains stable regardless of the value of the horizontal offset. When the flow rate crosses a critical value, the stability characteristics can suddenly change depending on the value of X_H/H. This phenomenon can be seen in Fig. 7(d)-(f) and Fig. 8(d)-(f). Consider a riser whose horizontal offset is zero or is given a small perturbation, i.e, the riser is nearly vertical, when the speed of the internal fluid is 80 m/s. This speed is intermediate between the first critical speed (61.1 m/s) and the second critical speed (80.5 m/s). As can be seen from Fig. 7(d) and Fig. 8(d), only the first mode becomes unstable. Then, when $V_i = 100$ m/s, which is right before the frequency of the fourth bending mode becomes zero (when $V_i = 100.4$ m/s), the first and

[4]It should be noted that the dimensionless horizontal offset $X_H/H = 0.38$ is the largest offset that can sustain the prescribed value of top tension ($T_{Top} = 476.2kN$). For offsets larger than 0.38, no static configurations are possible because the prescribed top tension value is below the critical top tension (T_{Cr}) for the riser. For additional details on this matter, see Kim and O'Reilly (2019a), and Chucheepsakul and Monprapussorn (2001).

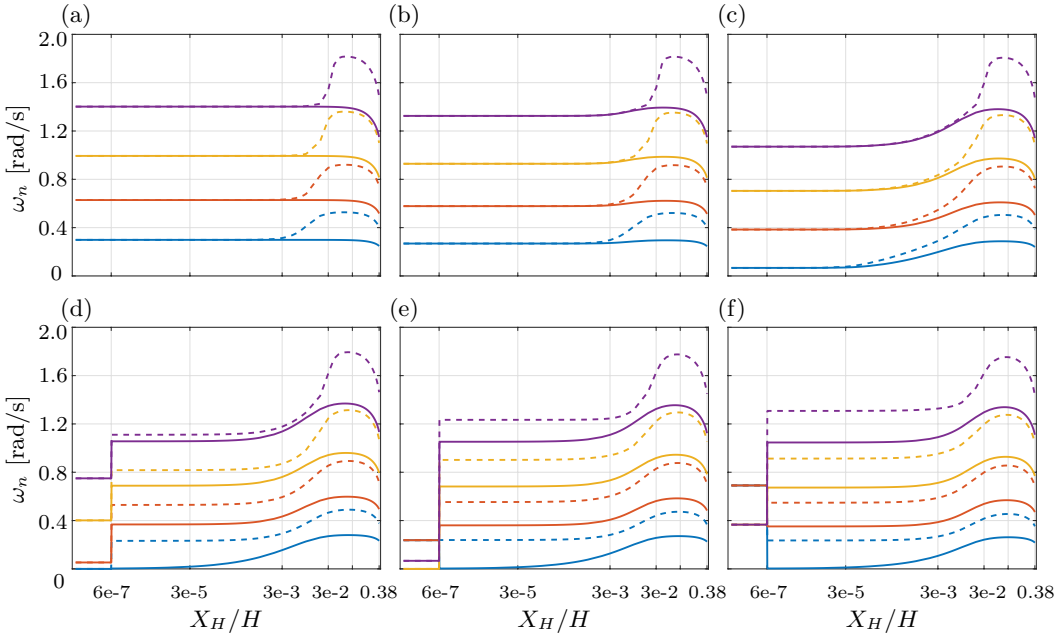

Fig. 7. The variations of the natural frequencies (ω_n) of the lowest four bending modes as a function of the dimensionless horizontal offset X_H/H for various values of the internal fluid transport speed V_i: (a) 0; (b) 30; (c) 60; (d) 80; (e) 100; and (f) 120 m/s. The solid lines show the out-of-plane bending modes in the Z-direction, while the dashed lines show the in-plane bending modes on the YZ plane.

the second mode are unstable, the third mode is unstable, and only the fourth mode is stable (Fig. 8(e)). In the end, when $V_i \approx 120$ m/s, the first and the second mode merge and the third and the fourth mode combine and all of the four modes are unstable (Fig. 8(f)). Even at these large values of V_i, however, as long as the riser configurations are not vertical, i.e., $X_H/H > 6 \times 10^{-7}$, then the riser will remain stable.

5. Conclusions

In this paper, the change in the stability characteristics of a riser as the horizontal offset X_H and transport speed V_i were varied was discussed. The top tension remained constant during these variations and, thus, the undeformed length of the riser was also varied. The riser was modeled using Kirchhoff's rod theory and is able to accommodate bending, torsional, and extensional deformations. In addition, fluid-structure interactions including internal fluid transport and buoyancy were accounted for in the model. The model and the numerical methods used to determine the static configuration and dynamic response were also validated with published results from the literature.

As the horizontal offset is increased from zero, the shape of the static configuration of the riser changes from vertical to catenary-like. In addition, the out-of-plane modes and in-plane modes start to show distinct behaviors. By analyzing the changes to the static configurations and dynamic characteristics, we are able to demonstrate how the instability associated with a critical transport speed vanishes when the offset X_H/H becomes

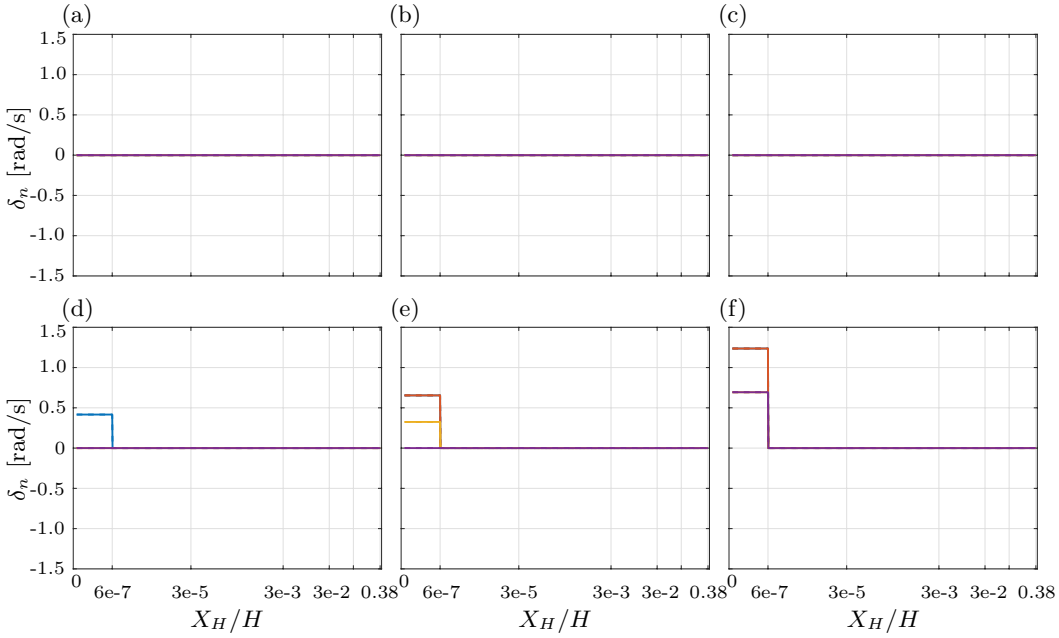

Fig. 8. The variations of the real parts of the eigenvalues (δ_n) of the lowest four bending modes as a function of the dimensionless horizontal offset X_H/H for various values of internal fluid transport speed (V_i): (a) 0; (b) 30; (c) 60; (d) 80; (e) 100; and (f) 120 m/s. The solid lines show the out-of-plane bending modes in Z direction, while the dash lines show the in-plane bending modes on YZ plane.

greater than 6×10^{-7}. That is, when the hang-off point is given a finite displacement from zero.

From the free-vibration analysis about a static configuration, we presented the variation of the out-of-plane and in-plane bending modes to quasistatic variations in both the transport speed of the internal fluid as well as the horizontal offset. These results are graphically summarized in Fig. 9. Results pertaining to small ($< 6 \times 10^{-7}$) values of X_H/H in this figure should be interpreted as perturbations to the hang-off point and thus stability results for the vertical riser. With this in mind, the results summarize the instability of the vertical riser as the transport speed V_i is increased and the stability of the catenary-type riser and its concomitant finite value of X_H/H regardless of the value of V_i. The stability results for the catenary-type riser are consistent with the results reported in Kim and O'Reilly (2019a).

The fact that the vertical riser can be stabilized by simply giving a finite horizontal displacement to the hang-off point is reminiscent of a similar phenomenon for a loaded column. An initially straight vertical column that is fixed at one end and loaded with a compressive vertical force buckles when the load exceeds a critical value (buckling load). However, it is possible to give the column an initial curvature and in so doing buckling can be avoided. An application of this result to the spinal column is presented in Lotz et al. (2012). These authors also interpret the introduction of curvature as an unfolding parameter for a pitchfork bifurcation. Such an interpretation can also be applied to the vertical riser by considering the horizontal offset as a unfolding parameter.

From our work, we conclude that both divergence and flutter type instabilities take place in the vertical riser transporting fluid when the fluid transport speed reaches critical values. A small horizontal offset separates the out-of-plane and in-plane bending modes and enables the riser to avoid the instability regardless of the magnitude of the fluid transport speed. We also confirmed that flexible risers with a considerable offset remain stable, regardless of the transport speed of the internal fluid, so long as the static configuration satisfies a certain criterion[5]. Our principal results are expected to provide effective and useful guidelines regarding the stability of marine flexible risers.

[5]As discussed in our earlier work (Kim and O'Reilly (2019a), the prescribed top tension should not be below the critical top tension, and the static configuration of interest should be the shorter of the two possible configurations that can exist with the same value of the top tension.

Reference

Alfosail, F. K., Nayfeh, A. H., Younis, M. I., 2017. Natural frequencies and mode shapes of statically deformed inclined risers. International Journal of Non-Linear Mechanics 94, 12–19.
URL https://doi.org/10.1016/j.ijnonlinmec.2016.09.007

Antman, S. S., 2005. Nonlinear Problems of Elasticity, 2nd Edition. Vol. 107 of Applied Mathematical Sciences. Springer-Verlag, New York.
URL http://dx.doi.org/10.1007/0-387-27649-1

Atanackovic, T., 1997. Stability Theory of Elastic Rods. World Scientific.
URL https://doi.org/10.1142/9789812819673

Bylsma, R., Ai, N., Van Baak, D., 1988. Oscillations of a suspended chain. American Journal of Physics 56 (11), 1024–1032.
URL https://doi.org/10.1119/1.15384

Chang, G. H., Modarres-Sadeghi, Y., 2014. Flow-induced oscillations of a cantilevered pipe conveying fluid with base excitation. Journal of Sound and Vibration 333 (18), 4265–4280.
URL https://doi.org/10.1016/j.jsv.2014.03.036

Chatjigeorgiou, I. K., Oct. 2010. On the effect of internal flow on vibrating catenary risers in three dimensions. Engineering Structures 32 (10), 3313–3329.
URL https://doi.org/10.1016/j.engstruct.2010.07.004

Chucheepsakul, S., Monprapussorn, T., 2001. Nonlinear buckling of marine elastica pipes transporting fluid. International Journal of Structural Stability and Dynamics 1 (03), 333–365.
URL https://doi.org/10.1142/S0219455401000263

Chucheepsakul, S., Monprapussorn, T., Huang, T., 2003. Large strain formulations of extensible flexible marine pipes transporting fluid. Journal of Fluids and Structures 17 (2), 185–224.
URL https://doi.org/10.1016/S0889-9746(02)00116-0

Eroglu, U., Tufekci, E., 2018. Small-Amplitude free vibrations of straight beams subjected to large displacements and rotation. Applied Mathematical Modelling 53, 223–241.
URL https://doi.org/10.1016/j.apm.2017.08.028

Ibrahim, R., 2010. Overview of mechanics of pipes conveying fluids Part I: Fundamental studies. Journal of Pressure Vessel Technology 132 (3), 034001.
URL http://doi.org/10.1115/1.4001271

Ibrahim, R., 2011. Mechanics of pipes conveying fluids Part II: Applications and fluidelastic problems. Journal of Pressure Vessel Technology 133 (2), 024001.
URL http://doi.org/10.1115/1.4001270

Kim, H.-T., O'Reilly, O. M., 2019a. Instability of catenary-type flexible risers conveying fluid in subsea environments. Ocean Engineering 173, 98–115.
URL https://doi.org/10.1016/j.oceaneng.2018.12.042

Kim, H.-T., O'Reilly, O. M., 2019b. On the effects of a buoyancy module on the dynamics of flexible risers transporting fluid. In: the 29th International Offshore and Polar Engineering Conference, 11-16 June, Honolulu, HI, USA. The International Society of Offshore and Polar Engineers, p. in press.
URL https://doi.org/TBD

Klaycham, K., Athisakul, C., Chucheepsakul, S., Jun. 2017. Nonlinear vibration of marine riser with large displacement. Journal of Marine Science and Technology 22 (2), 361–375.
URL http://doi.org/10.1007/s00773-016-0416-8

Lotz, J. C., O'Reilly, O. M., Peters, D. M., 2012. Some comments on the absence of buckling of the ligamentous human spine in the sagittal plane. Mechanics Research Communications 40, 11–15.
URL https://doi.org/10.1016/j.mechrescom.2011.11.010

Love, A. E. H., 1927. A Treatise on the Mathematical Theory of Elasticity, 4th Edition. Cambridge University Press, Cambridge.

Monprapussorn, T., Athisakul, C., Chucheepsakul, S., 2007. Nonlinear vibrations of an extensible flexible marine riser carrying a pulsatile flow. Journal of Applied Mechanics 74 (4), 754–769.
URL https://doi.org/10.1115/1.2711226

Morison, J., Johnson, J., Schaaf, S., 1950. The force exerted by surface waves on piles. Journal of Petroleum Technology 2 (5), 149–154.
URL https://doi.org/10.2118/950149-g

Neukirch, S., Frelat, J., Goriely, A., Maurini, C., 2012. Vibrations of post-buckled rods: the singular inextensible limit. Journal of Sound and Vibration 331 (3), 704–720.
URL https://doi.org/10.1016/j.jsv.2011.09.021

Ni, Q., Zhang, Z., Wang, L., 2011. Application of the differential transformation method to vibration

analysis of pipes conveying fluid. Applied Mathematics and Computation 217 (16), 7028–7038.
URL https://doi.org/10.1016/j.amc.2011.01.116

O'Reilly, O. M., 2017. Modeling Nonlinear Problems in the Mechanics of Strings and Rods. Springer-Verlag, New York.
URL http://dx.doi.org/10.1007/978-3-319-50598-5

Païdoussis, M. P., 1966. Dynamics of flexible slender cylinders in axial flow Part 1. Theory. Journal of Fluid Mechanics 26 (4), 717–736.
URL https://doi.org/10.1017/S0022112066001484

Païdoussis, M. P., 1975. Flutter of conservative systems of pipes conveying incompressible fluid. Journal of Mechanical Engineering Science 17 (1), 19–25.
URL https://doi.org/10.1243/JMES_JOUR_1975_017_005_02

Païdoussis, M. P., 2014. Fluid-Structure Interactions, Slender Structures and Axial Flow. Vol. 1. Academic Press, San Diego, California, USA.
URL https://doi.org/10.1016/c2011-0-08057-2

Païdoussis, M. P., 2016. Fluid-Structure Interactions, Slender Structures and Axial Flow. Vol. 2. Academic Press, Kidlington, Oxford, U.K.
URL https://doi.org/10.1016/C2011-0-08058-4

Ritto, T., Soize, C., Rochinha, F., Sampaio, R., 2014. Dynamic stability of a pipe conveying fluid with an uncertain computational model. Journal of Fluids and Structures 49, 412–426.
URL https://doi.org/10.1016/j.jfluidstructs.2014.05.003

Santillan, S. T., Virgin, L. N., Plaut, R. H., 2010. Static and dynamic behavior of highly deformed risers and pipelines. Journal of Offshore Mechanics and Arctic Engineering 132 (2), 021401.
URL http://dx.doi.org/10.1115/1.4000555

Sazesh, S., Shams, S., 2019. Vibration analysis of cantilever pipe conveying fluid under distributed random excitation. Journal of Fluids and Structures 87, 84–101.
URL https://doi.org/10.1016/j.jfluidstructs.2019.03.018

Shampine, L. F., Gradwell, I., Thompson, S., 2003. Solving ODEs with MATLAB. Cambridge University Press, Cambridge.
URL http://dx.doi.org/10.1017/cbo9780511615542

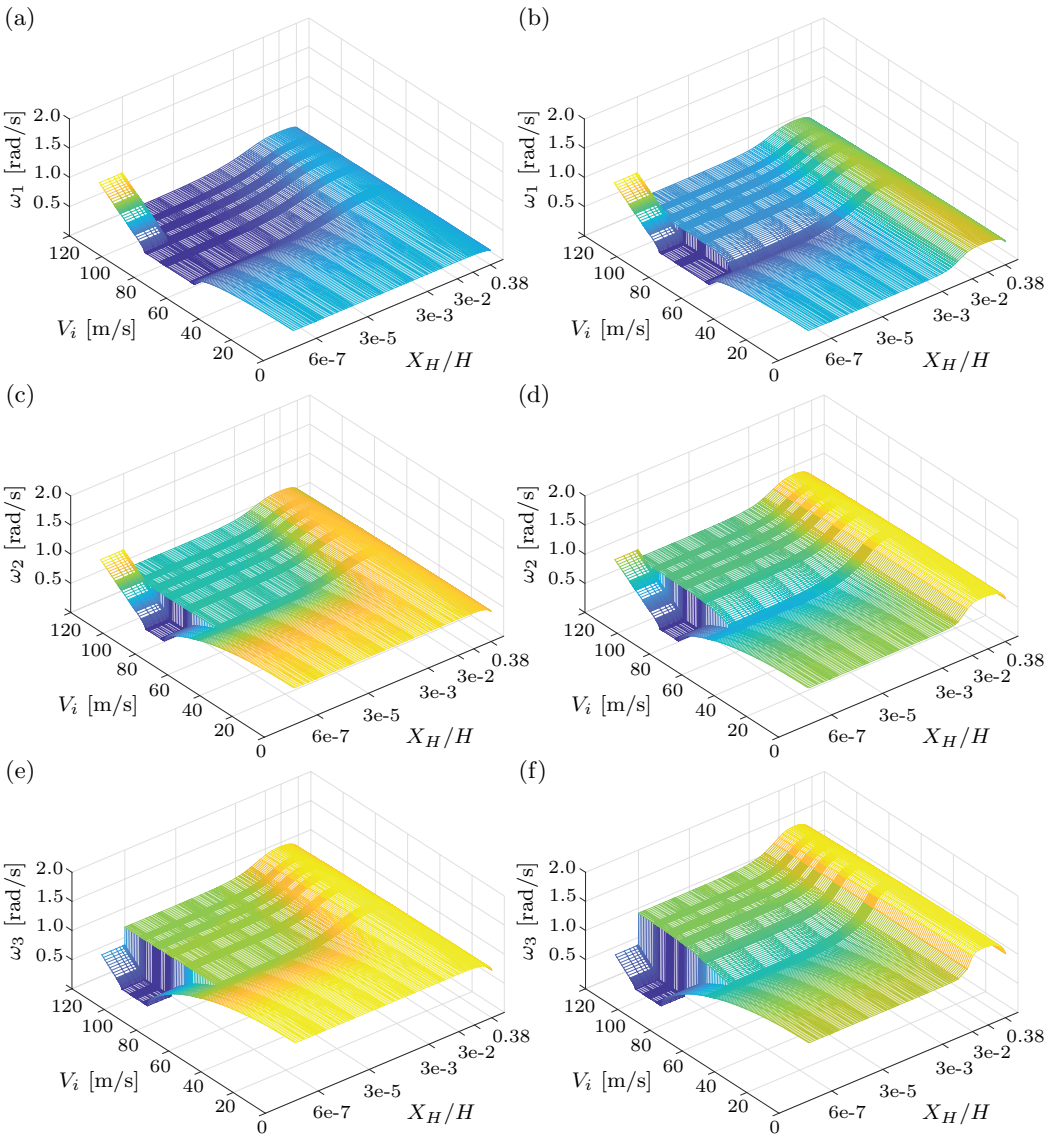

Fig. 9. The variation of the lowest three out-of-plane ((a),(c), and (e)) and in-plane ((b), (d), and (f)) bending modes (ω_n, Z axis) along both the dimensionless horizontal offset (X_H/H, X axis) and the internal fluid speed (U, Y axis), displayed in three dimensional plot: (a) 1st out-of-plane bending mode; (b) 1st in-plane bending mode; (c) 2nd out-of-plane bending mode; (d) 2nd in-plane bending mode; (e) 3rd out-of-plane bending mode; and (f) 3rd in-plane bending mode.